

MICROBIAL JAROSITE AND GYPSUM FROM CORROSION OF PORTLAND CEMENT CONCRETE

KAZUE TAZAKI

Department of Geology, Shimane University, Matsue, Shimane 690, Japan

TADAHIRO MORI

Department of Biochemical Engineering, Shimane University, Matsue, Shimane 690, Japan

TSUGUHIRO NONAKA

Department of Agricultural Engineering, Shimane University, Matsue, Shimane 690, Japan

ABSTRACT

Jarosite $\text{KFe}_3(\text{SO}_4)_2(\text{OH})_6$ and gypsum $\text{CaSO}_4 \cdot 2\text{H}_2\text{O}$ have been found in a corroded concrete sewer pipe. The rate of corrosion of the concrete is calculated to be 4.3 to 4.7 mm/year along the inner surface of the pipe, at 25–30°C and H_2S concentrations up to 400 ppm in the atmosphere, under low-pH conditions. The number of *Thiobacillus thiooxidans* on the corroded surface was found to be 10^3 – 10^4 g^{-1} , and the C/N ratio after treatment with HCl was found to be 7–10, indicative of a high content of organic matter. TEM, SEM and EDAX studies reveal the mechanisms of crystal growth of jarosite and gypsum grown from rod or granule. TEM photographs show that embryonic matter coated with hydrated films is essentially crystalline, having layer spacings characteristic of jarosite and gypsum. There appears to be no morphological difference between jarosite and gypsum at the embryonic stage, but they have their own characteristic *d*-values. The amplitude of these phenomena depends upon the low pH of solution and the breakdown of cement concrete aided by the activity of *T. thiooxidans*. The deposition of jarosite and gypsum is stimulated by bacterial activity during the corrosion of Portland cement concrete.

Keywords: microbial jarosite, gypsum, corrosion, *Thiobacillus thiooxidans*, cement concrete.

SOMMAIRE

Nous décrivons la formation de jarosite $\text{KFe}_3(\text{SO}_4)_2(\text{OH})_6$ et de gypse $\text{CaSO}_4 \cdot 2\text{H}_2\text{O}$ dans les tuyaux d'égoûts de béton affectés par la corrosion. Le taux de corrosion du béton est de 4.3 à 4.7 mm par année le long de la paroi interne, à 25–30°C et des concentrations de H_2S atteignant 400 ppm dans l'atmosphère, à un faible pH. Le nombre de *Thiobacillus thiooxidans* sur la surface attaquée était de 10^3 à 10^4 g^{-1} , et le rapport C/N après traitement au HCl était de 7 à 10, preuve d'un contenu élevé de matière organique. Les études par microscopies électroniques à transmission et à balayage, et les résultats d'analyses par dispersion d'énergie, révèlent les mécanismes de croissance des cristaux de jarosite et gypse impliquant des bâtonnets et des granules recouvertes d'un liseré hydraté. A un stade embryonnaire, ce matériau, recouvert d'un film hydraté, est essentiellement cristallin, car il possède un espacement *d* typique de la jarosite ou du gypse. Il ne semble pas y avoir de différences morphologiques entre la jarosite et le gypse au stade embryonnaire, mais chacun possède ses propres espacements *d*. L'impact environnemental de ces phénomènes dépend du faible pH de la solution et de la déstabilisation du béton, accéléré par l'activité des bactéries *T. thiooxidans*. La formation de jarosite et de gypse embryonnaires serait stimulée par activité bactérienne pendant la corrosion du béton de Portland.

(Traduit par la Rédaction)

Mots-clés: jarosite microbienne, gypse, corrosion, *Thiobacillus thiooxidans*, béton.

INTRODUCTION

A large number of investigations into the formation of jarosite by the oxidation of pyrite have been summarized by Van Breemen (1988). The jarosite group of minerals generally occurs as a

yellow mottle or stains within acidic sulfate soils, and is due to *in situ* weathering of exposed sulfides (Michel & Van Everdingen 1987). The spontaneous microbial oxidation of iron in pyrite and marcasite to form various ferrous sulfates in soils and the contribution of the weathering process to the

formation of jarosite are well known (Ivarson *et al.* 1982). Occurrences of iron- and sulfur-bearing phases involved in the formation of acid sulfate soils have been described by Krumbain (1983), Van Breemen (1988), Silver *et al.* 1986, Krumbain & Dahanayake (1985), Wiese & Fyfe (1986), and Alpers *et al.* (1989). The jarosite group of hydrous iron sulfate minerals (*e.g.*, melanterite, szomolnokite, rozenite, coquimbite, roemerite) also commonly occurs as crusts or coatings related to oxidation of sulfide minerals (Brophy & Sheridan 1965). Experiments on the production of ferrous sulfates, iron sulfides, and iron oxides from ferrous sulfate solution under different conditions controlled by buffers (Al and Si) and pH have been described by Wiese *et al.* (1987), Beveridge *et al.* (1983) and Krishamurti & Huang (1989). The occurrence of jarosite formed from oxidation of sulfide minerals in northern Chile, California and Yukon also have been reported by Michel & Van Everdingen (1987), Alpers & Brimhall (1989) and Alpers *et al.* (1991). Zodrow & McCandlish (1978) suggested that bacterial activity aided the breakdown of pyrite under conditions of extremely low pH. According to the literature, the major micro-organisms involved in those reactions have been identified as *Thiobacillus ferrooxidans* or *Thiobacillus thiooxidans*. In this paper, we describe a major accumulation of jarosite and gypsum associated with the corrosion of Portland cement concrete. Transmission electron microscope (TEM) photographs have revealed details of these minerals for the first time at the ångström scale.

Even though much work has been done on the microbial corrosion of concrete (Parker 1945, Pomeroy 1970, Sand & Bock 1984, US EPA 1985, Sand 1987, Nielsen & Huvitved-Jacobsen 1988), the processes of mineral corrosion, environmental conditions, and the role of bacterial activity in the corrosion mechanism are not well understood. This paper reports the crystallization of jarosite and gypsum that is stimulated by bacterial activity during the corrosion of Portland cement concrete.

MATERIALS AND METHODS

The deterioration of concrete sewer pipes by expansion, cracking, loss of strength and stiffness was observed at the Ohmuta Drainage Treatment Plant, Japan (Mori *et al.* 1992). The sewer pipes, 1 m in diameter and 9 cm in thickness, have been corroding for 12 years in the presence of up to 400 ppm H₂S gas concentrations at temperature of 25–30°C. Under the microscope, the corroded part shows five distinct zones of secondary products, as shown in Figure 1. Thin sections and rough-cut surfaces of corroded walls of sewer pipe were observed with a Hitachi S-2100 scanning electron

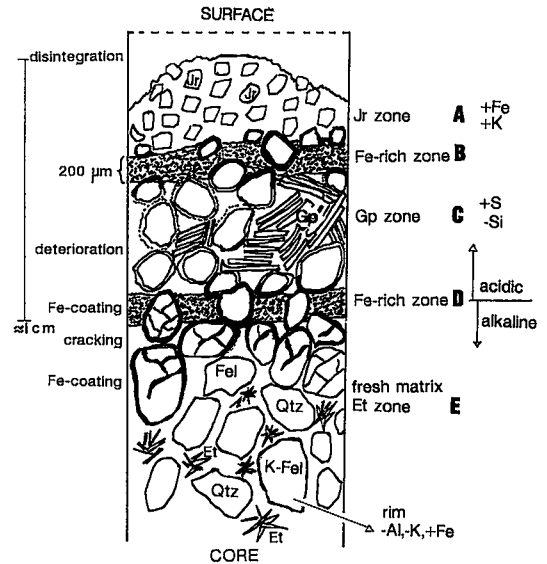


FIG. 1. Schematic mineralogy of corroded sewer pipes showing zonal formation of jarosite, gypsum and Fe-rich zone. Jr: jarosite, Gp: gypsum, Et: ettringite, Fel: feldspar, Qtz: quartz.

microscope (SEM) equipped with a Horiba EMAX 3000 energy-dispersion system, and a JEOL JSM-T220A SEM. Powder samples were studied using X-ray diffraction (Rigaku goniometer, CuK α radiation). The C, H and N contents of the powder samples were determined with a Yanaco MT-3 CHN-coder thermal conductivity detector based on the Pregl-Dumas method. Transmission electron microscopy (JEOL, JEM 2000EX) was used for the fine fraction of the suspension. The number of *Thiobacillus thiooxidans* existing in the corroded materials was determined using an AT medium (mixture of A and T solutions). The composition of the starting AT medium was as follows: NH₄Cl 0.5 g, KH₂PO₄ 4.0 g, K₂HPO₄ 4.0 g, MgSO₄•7H₂O 0.8 g, EDTA 0.5 g, ZnSO₄•7H₂O 0.22 g, CaCl₂ 0.0544 g, MnCl₂•4H₂O 0.0506 g, FeSO₄•7H₂O 0.0499 g, (NH₄)₆Mo₇O₂₄•4H₂O 0.011 g, CaSO₄•5H₂O 0.0157 g, CoCl₂•6H₂O 0.0161 g, water 1 L, and pH 7.0. Corrosion was studied during five months at room temperature, and at H₂S concentration of about 400 ppm. *T. thiooxidans* isolated from corroded materials in the concrete sewer pipe was inoculated on the surface of the mortar specimen every two weeks for the first two months of the experiment. Quantification and determination of *T. thiooxidans* were made following procedures by Santer *et al.* (1959) and Mori *et al.* (1992). The pH of the corroded materials was

determined using a pH meter (Horiba M-8) after these materials were suspended in distilled water. A mortar specimen also was studied for comparison with Portland cement concrete in the laboratory.

RESULTS

XRD results

The jarosite zone A in Figure 1, in yellow to white colors, was found to be the most strongly corroded. X-ray powder diffraction of the products of corrosion within 1 cm from the wall surface (Fig. 1, zone A-D) shows the presence of gypsum, jarosite and quartz (Fig. 2). The d values of 7.83, 4.33 and 3.85 Å are characteristic peaks of gypsum, whereas those at 6.11, 5.79, 5.19 and 3.143 Å are characteristic peaks of jarosite. The strongest intensity peak of jarosite at 3.099 Å (113) overlaps with a gypsum peak (141). These spacings are slightly larger than for the standard minerals because of substitution of H_3O^+ for K^+ , which affects both a and c cell dimensions in jarosite (Alpers *et al.* 1991). The d value at 4.33 Å for gypsum overlaps with a quartz peak; as result, the intensity is higher than that of the 7.83 Å peak ($I=100$) of gypsum. Gypsum and jarosite are secondary products that result from the reaction between H_2SO_4 and the concrete sewer pipe, whereas quartz is one of the primary components

of the concrete. Ettringite $\text{Ca}_6\text{Al}_2(\text{SO}_4)_3(\text{OH})_{12}\cdot 25\text{H}_2\text{O}$ or $\text{Ca}_4\text{Al}_2(\text{SO}_4)(\text{OH})\cdot 2\text{H}_2\text{O}$ and clay minerals were not seen in these zones. In case of the most corroded mortar bar, secondary ettringite was produced with gypsum, calcite and barite, but without jarosite.

SEM-EDAX results

The well-formed crystals of jarosite found on the corroded wall of sewer pipe have a rhombohedral form (1-2 μm across). They contain, in addition to high concentrations of S, Fe and K, traces of Al, Si, and Ca (Fig. 3). The Al may be present in jarosite structure as a solid-solution component in view of the unit-cell dimensions of jarosite calculated from the XRD results. Prismatic crystals, 0.1 to 0.5 μm wide and 0.5 to 5 μm long, occur below the jarosite zone (Fig. 4). These are rich in S and Ca, with small amounts of Al, K and Fe, and are interpreted as being gypsum. A strong Si signal is interpreted to reflect the presence of quartz as a primary component of the concrete. A small amount of jarosite is responsible for the weak peaks of K and Fe in the EDAX pattern.

Analysis of microbes and organic matter

The area around the sewage level was most strongly corroded, and the corrosion rates were

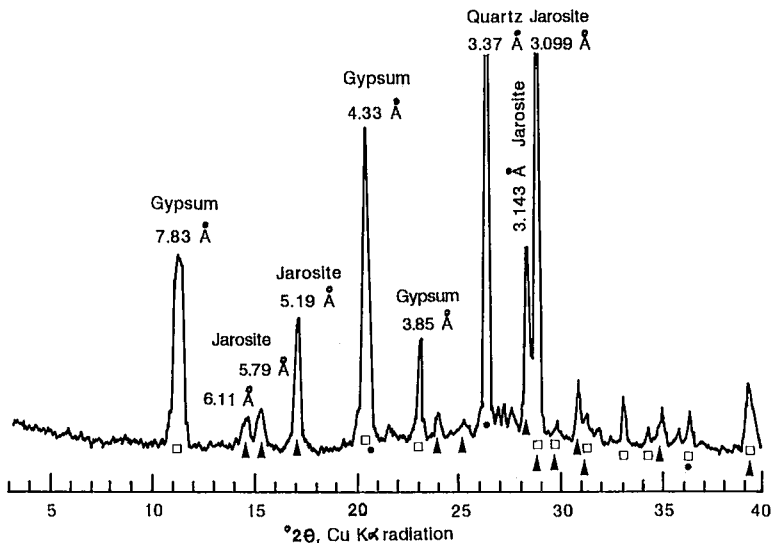


FIG. 2. X-ray powder-diffraction patterns of the most strongly corroded part of the sewer pipe. Material taken from the interval 0-1 cm shows gypsum (open square), jarosite (triangle), and quartz (circle).

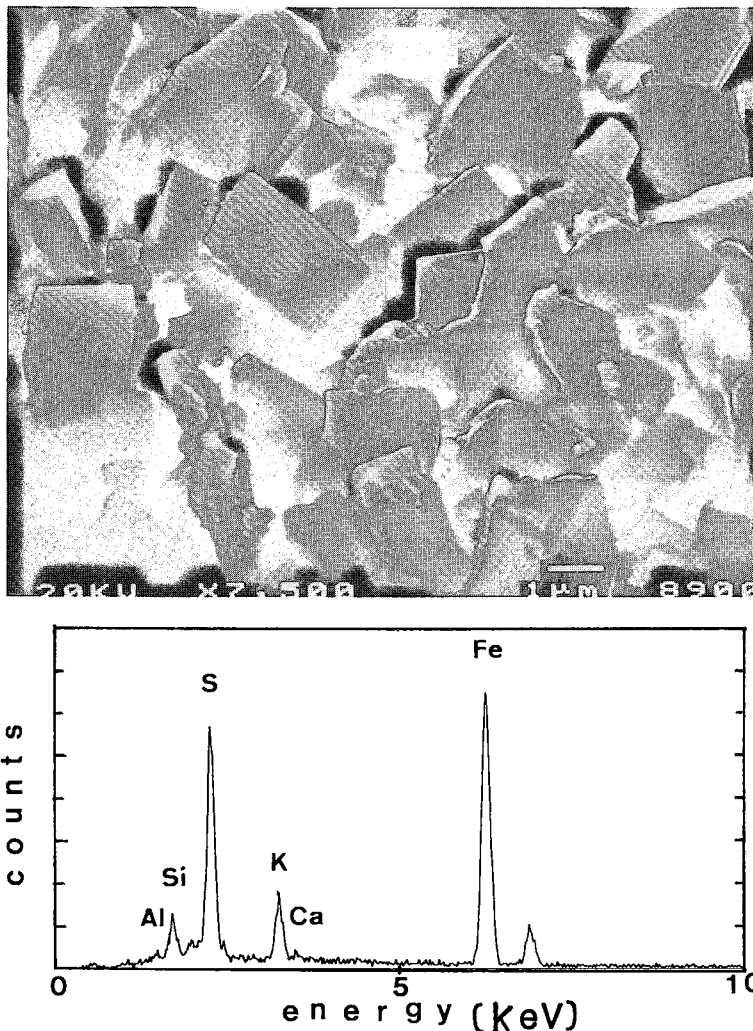


FIG. 3. Scanning electron micrograph of rhombs of jarosite and its elemental composition by energy-dispersion analysis.

found to decrease with distance from the water level. The highest rates of corrosion by the sewage were found to be 4.7 mm per year over the 32 mm depth from the surface of pipe wall, exposed for 12 years. The corrosion rate at the top of the pipe was 1.4 mm per year, approximately 1/3 of the rate at the sewage level. The numbers of *T. thiooxidans* existing in the corroded parts (0–11 mm) were 10^3 – 10^4 per gram (Table 1). The corroded part was found to contain 0.95–1.55% hydrogen, 0.38–1.57% carbon, and 0.04–0.23% nitrogen. The C/N ratio was found to be 6.69–9.88 after treatment with HCl (Table 2). In the case of

a low level of organic components, the C/N ratio is about 11.0, with reference to a value for distilled water (Sampei 1991). The C/N ratio and the number of *T. thiooxidans* in the corroded parts provide indications of high levels of organic components and high microbial activity.

A suspension of a mixture of 1 g of corroded materials with 1 g of distilled water indicates a low pH (3.2–4.0), whereas the fresh parts of cement concrete show a high pH, between 11.6 and 12.0. The rate of production of H_2S from the sludge ranged from 5.5 to 64 $\mu g H_2S/g\text{-solid}\cdot hr$ (Mori *et al.* 1992). The rate of production of H_2S depends

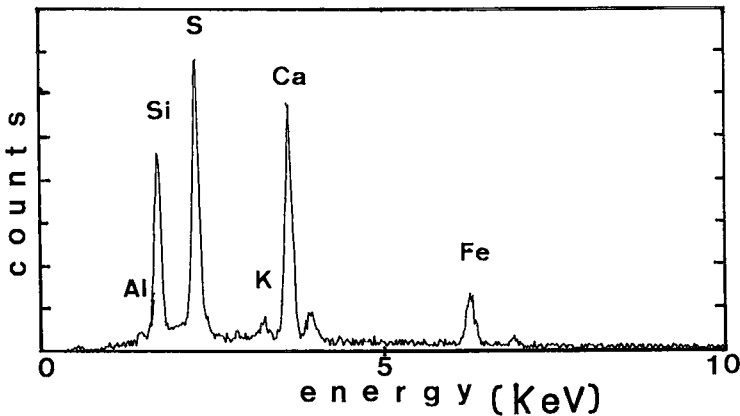
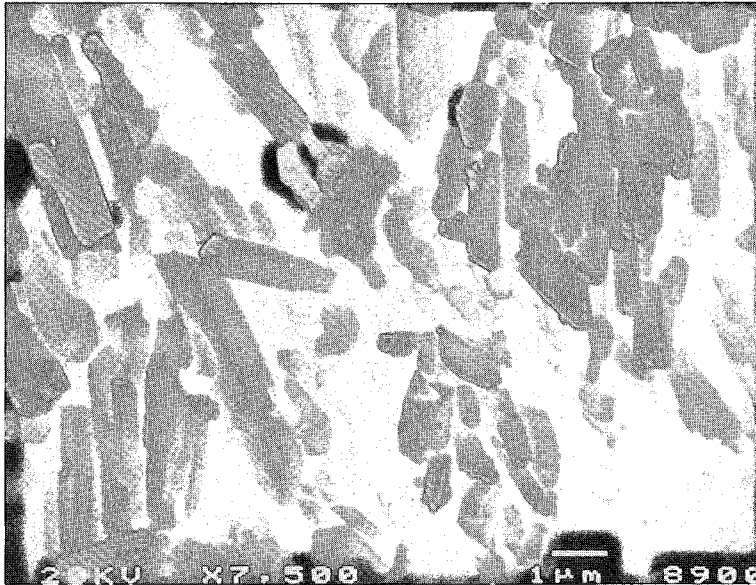


FIG. 4. Scanning electron micrograph of lath-shaped gypsum and its elemental composition by energy-dispersion analysis.

on the content of organic components and the number of sulfate-reducing bacteria (SRB) in the sludge.

T. thiooxidans was experimentally inoculated on the surface of a mortar specimen (Mori *et al.* 1992) for two months for comparison with the Portland cement concrete. The mortar specimens were corroded about 20 mm in thickness within 40 mm total thickness above the liquid level in sewage 50 mm deep or the AT medium (Tazaki *et al.* 1990b). The mortar specimens kept in the distilled water did not become corroded. Thus, the inoculated *T. thiooxidans* had attacked the mortar surface, and

had increased the numbers of *T. thiooxidans* in the corroded materials.

T. thiooxidans from the corroded Portland cement concrete was cultivated on an AT medium. The elongate and rod-shaped cell of *T. thiooxidans*, 1–2 μm long and 0.3–1.0 μm wide, are connected to each other (Fig. 5). Organic materials are ringed and precipitated on the bacterial body (Figs. 6A, B). Rhombohedral crystals of jarosite were formed with *T. thiooxidans* (Fig. 7A). The small jarosite crystals are connected to each other by hydrated thin films and have grown into large-size rhombohedral crystals around *T. thiooxidans* (Fig. 7B).

TABLE 1. NUMBER OF *Thiobacillus thiooxidans* AND SUSPENSION pH

Depth from surface (cm)	<i>T. thiooxidans</i> g ⁻¹	pH in the suspension	H ₂ O wt %
0 - 0.4	9.7 × 10 ⁴	3.2	20.8
0.4 - 0.9	9.6 × 10 ⁴	3.5	18.1
0.9 - 1.1	3.1 × 10 ³	4.0	5.2
1.1 - 2.6	0	11.6 - 12.0	2.0
2.6 - 4.1	0	11.6 - 12.0	0.7
4.1 - 5.6	0	11.6 - 12.0	0.7
5.6 - 7.1	0	11.6 - 12.0	1.2

The corroded sewer pipe shows a sharp boundary between fresh concrete (under 1.1 cm) and corroded parts (above 1.1 cm).

TABLE 2. RESULTS OF CHEMICAL ANALYSES OF THE MOST CORRODED PARTS OF THE SEWER PIPES

Sample	Untreated				Treated with HCl			
	H %	C %	N %	C/N	H %	C %	N %	C/N
1-0-1	1.19	1.52	0.21	7.27	0.95	1.57	0.23	6.69
1-0-2	1.70	0.42	0.06	6.77	1.55	0.38	0.04	9.88

Results quoted in wt. %.

TEM results

TEM observations reveal evidence of a role of microbes in the formation of jarosite and gypsum in the corroded cement concrete, as shown in Figures 8-10. The embryonic stages of biomineralization have been revealed by TEM studies. Rod-shaped material (200 nm long) with thin films (Fig. 8, left side) and granular or polygonal materials are present (Fig. 8, arrow). The thin films are easily damaged by the electron beam, and dehydrate after long exposure. The material appears to be opaque because of hydrolysis of Fe³⁺ in jarosite to make Fe(OH)₃. The Mössbauer spectrum of the sample at room temperature indicates that at least two forms of iron (Fe²⁺ and Fe³⁺) are present.

Lattice fringes of 3.7, 4.2 and 6.3 Å can be seen in the rod and granular or polygonal crystals associated with hydrated films (Fig. 9). In the thick hydrated films, the lattice images of the rod were not evident because of the high optical density. Holes in the hydrated films are due to dehydration during observation (Fig. 9B). The 3.7 and 4.2 Å *d* values correspond to (110) of jarosite and (12 $\bar{1}$) of gypsum, respectively. The 6.3 Å *d* value probably corresponds to the second order of (021) or (113) of jarosite. The embryonic morphologies of the polygonal and the rod shapes seem to be jarosite (Fig. 9A) and gypsum (Fig. 9B), respectively.

Figure 10A clearly shows evidence of crystal

growth of gypsum, having a 3.8 Å (031, 040) value. The boundary of the division is not sharp; it shows 3.8 Å lattice fringes. The undulatory rim of the rod is due to dehydration. The 3.8 Å lattice grew oblique to the axis of elongation (Fig. 10A), whereas the 5.7 Å lattice grew parallel to the long axis of the rod (Fig. 10B). The 5.7 Å spacing corresponds to (003) of jarosite.

Many embryonic growth forms of crystals were observed, as schematically summarized in Figure 11. These embryonic or precursor products from corroded concrete are essentially crystalline, approximately 2000-3000 Å long and 200-500 Å wide. All lattice images obtained by TEM observation are closely related to the structure of gypsum and jarosite. These crystals have coalesced to form chains that show fission-like features of cell walls of the replaced bacterial materials, suggesting that bacterial activity aided the formation of jarosite and gypsum.

DISCUSSION

Role of biological factors for jarosite formation

Bloomfield & Coulter (1973), Ivarson (1973), Torma (1976), Tuovinen & Carlson (1979) and Alpers *et al.* (1989, 1991) found that jarosite and *T. ferrooxidans* are present in acid sulfate soils at pH 4 where K, Na and NH₄ are available in the system. Jarosite-type minerals are basic ferric sulfates and may be represented as AFe₃(SO₄)₂(OH)₆, where A represents K⁺, NH₄⁺, Na⁺ or H₃O⁺. Ivarson *et al.* (1978, 1979, 1980) examined the role that *T. ferrooxidans* in the formation of acid sulfate soils. A solution of FeSO₄ (pH 3.6) containing either minerals or alkali cations (K, NH₄ and Na) inoculated with *T. ferrooxidans* were cultivated for periods of up to 451 days. They found that in all inoculated systems, Fe²⁺ was oxidized, and H₂SO₄ was formed. Jarosite can be synthesized within 1-6 months at room temperature by aerating solutions of FeSO₄ and K₂SO₄ at pH 1-2. If *T. ferrooxidans* is present in such solutions, jarosite can be formed within days (Ivarson *et al.* 1982). *T. ferrooxidans* is able to oxidize Fe²⁺ at a rate 600 to 500,000 times faster than would occur in its absence (Lacey & Lawson 1970, Ivarson & Sojak 1978). The acid-tolerant *T. ferrooxidans* accelerates oxidation of dissolved Fe²⁺ to Fe³⁺ by five to six orders of magnitude and is able to maintain a steady-state concentration of Fe³⁺. The importance of the catalytic effects of the Fe³⁺ - *T. ferrooxidans* couple is well established for acid mine-drainage, where the pH commonly drops below 3 (Nordstrom 1982, Taylor *et al.* 1984). *T. ferrooxidans* bacteria were identified in the formation of jarosite around the cell wall (Fig. 7B).



FIG. 5. Transmission electron micrograph of cultivated *T. thiooxidans* isolated from corroded sewer pipe at 30°C for 2 weeks using the AT medium. *T. thiooxidans* bacteria join at the arrow by a thin film.

In the corroded Portland cement concrete of the present study, the high C-H-N contents and a high number of *T. thiooxidans* bacteria have strongly indicated formation of sulfur-bearing minerals, resulting from bacterial reduction of sulfate. The formation of jarosite is regarded not only to favor feldspar dissolution (Tazaki *et al.* 1990a), but also to promote the formation of carbohydrate-like compounds produced by bacterial action in the corroded cement concrete. The rates of H₂S production were found to range from 5.5 to 6.4 µg H₂S/g-solid.hr, depending on the content of organic compounds and number of sulfate-reducing bacteria (SRB) (Mori *et al.* 1992). In their

laboratory experiments, *T. thiooxidans* was inoculated on the surface of a mortar specimen. The nutrients in sewage stimulated the formation of sulfate by *T. thiooxidans* and accelerated corrosion. The results indicate that the mechanism of jarosite formation in the corroded cement concrete is similar to that responsible for the formation of jarosite, which was accelerated by *T. ferrooxidans* in acid sulfate soils.

Processes of zonal corrosion

The phenomenon of concrete corrosion seems to have a large effect on the geochemical and

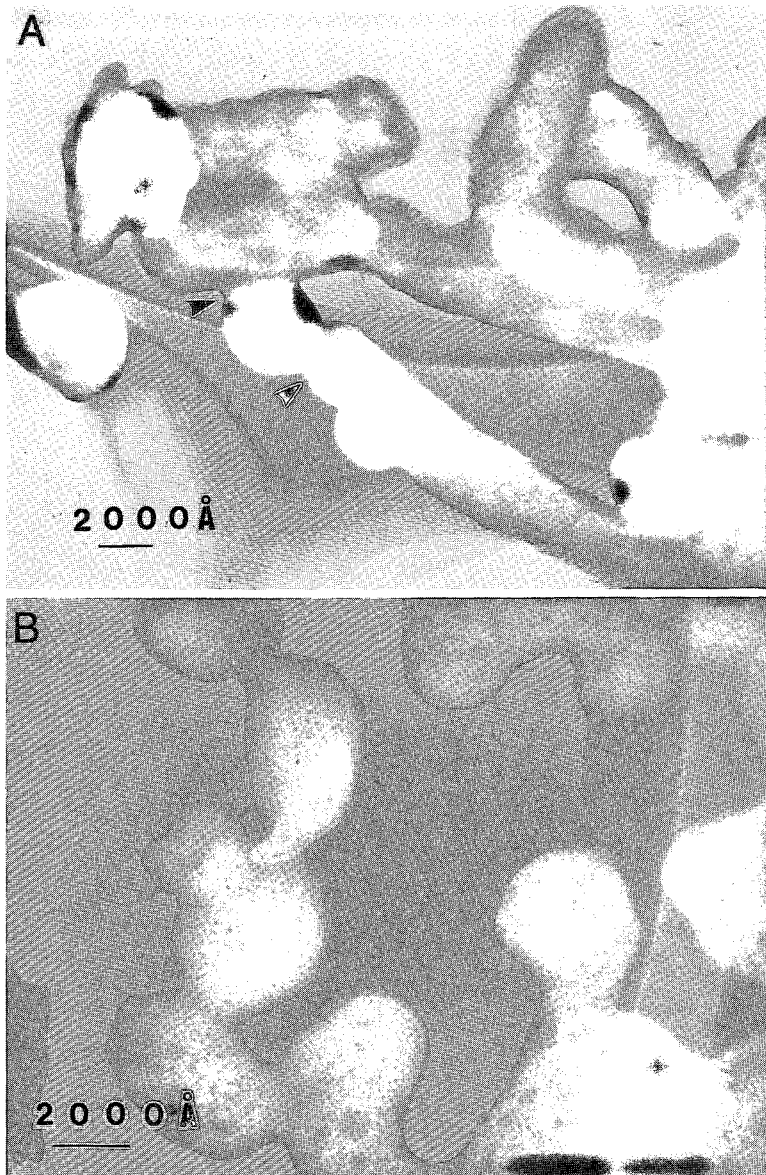


FIG. 6. Transmission electron micrographs of cultivated *T. thiooxidans* with organic materials around the cell (arrows in A) and tied in a row (B).

biochemical cycle of Fe, K, S and Ca, with bacteria involved in dissolution and precipitation processes. As shown in Figure 1, evidence of zonal corrosion can be seen: 1) Starting with the ettringite zone E: the pH remained alkaline (pH 11.6-12.0), and *T. thiooxidans* did not exist in this zone. 2) Cracking concrete with Fe-coating in zone D: the iron oxide

is known to be resistant to sulfate attack. The pH changes to acidic from alkaline. 3) Attack and deterioration of concrete: acidic conditions of pH 3-4, relatively high percentages of moisture, and *T. thiooxidans* were present at this level. Sulfur concentration increases, whereas silica concentration decreases. 4) Formation of gypsum in zone C:

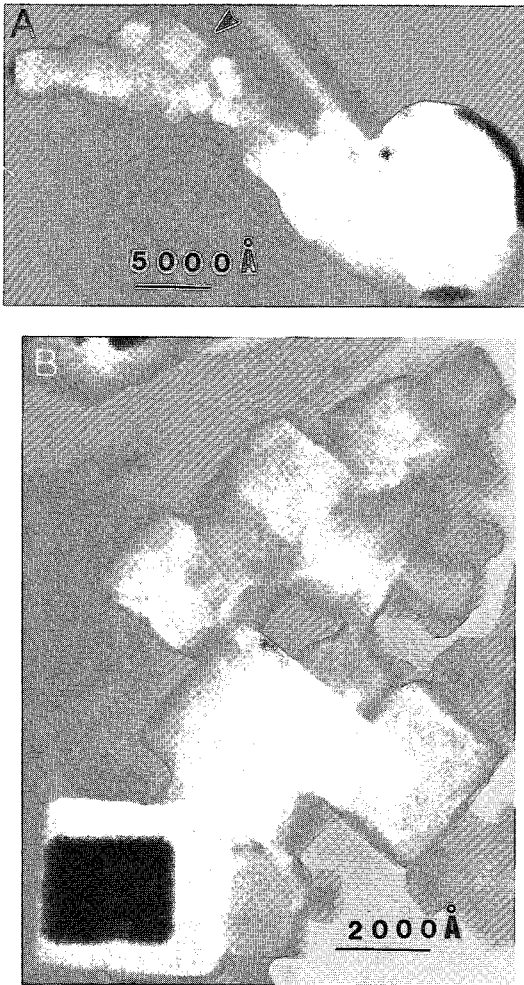


FIG. 7. Transmission electron micrographs of cultivated *T. thiooxidans* (A) tied in a row of rhombs of jarosite around the cell of *T. ferrooxidans* (B). The small rhombohedral crystals are connected and grow into large crystals (B).

the formation of gypsum is closely connected with the composition of the sulfate solution entering this level. *T. thiooxidans* and *T. ferrooxidans* promote catalytic bacterial reactions. 5) Precipitation of Fe-rich zone B: the oxidation of Fe appears to occur later, as existing sulfates are exposed to the atmosphere (Wiese *et al.* 1987). Solubility of iron sulfate is dependent on the low pH and acid attack on concrete (Moum & Rosenqvist 1959). Below a pH of 3 or 4, much stronger and quicker action of sulfate occurs on concrete containing insoluble ferrihydrite. 6) Formation of jarosite in zone A:

the greatest rates of corrosion occurred at the sewage level (zone A) because of the presence of moisture, nutrients, H_2S and HS^- . This level is a suitable area for the growth of *T. thiooxidans* and *T. ferrooxidans* under strongly acidic conditions. The formation of jarosite, $KFe_3(SO_4)_2(OH)_6$, as a result of reaction between sulfate and hydration products of Portland cement was found at this level. The relevant chemical reaction for the formation of jarosite is: $K^+ + 3Fe^{3+} + 2SO_4^{2-} + 6H_2O \rightarrow KFe_3(SO_4)_2(OH)_6 + 6H^+$.

The sulfide may undergo oxidation several times in zones A–C, steadily destroying the concrete, which forms a primary precipitation of ferrihydrite, gypsum and jarosite.

TEM observations

TEM affords the high resolution required to follow the crystallization of jarosite and gypsum in the presence of bacteria. There are numerous reports in literature of corrosion of concrete by micro-organisms, but most studies are at the optical or SEM level (Leadbeater & Riding 1986, Wiese *et al.* 1987). Using TEM, we have outlined processes of crystallization of jarosite and gypsum that are involved in the microbial corrosion of Portland cements. TEM photographs show that the

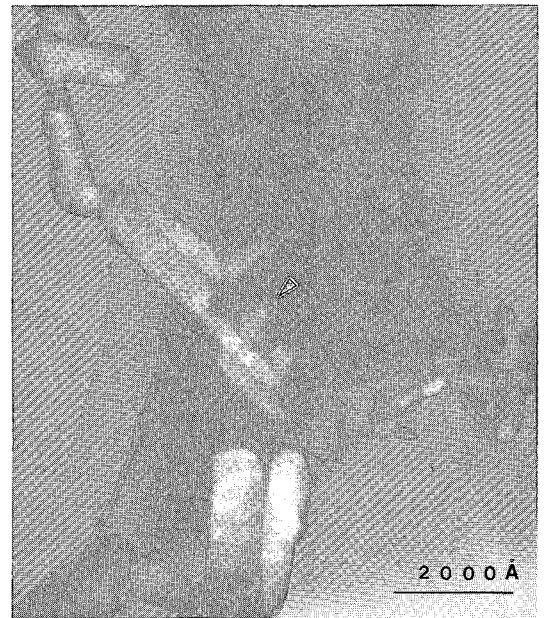


FIG. 8. Transmission electron micrograph of embryonic jarosite and gypsum crystals, showing division patterns of a rod-shaped crystal.

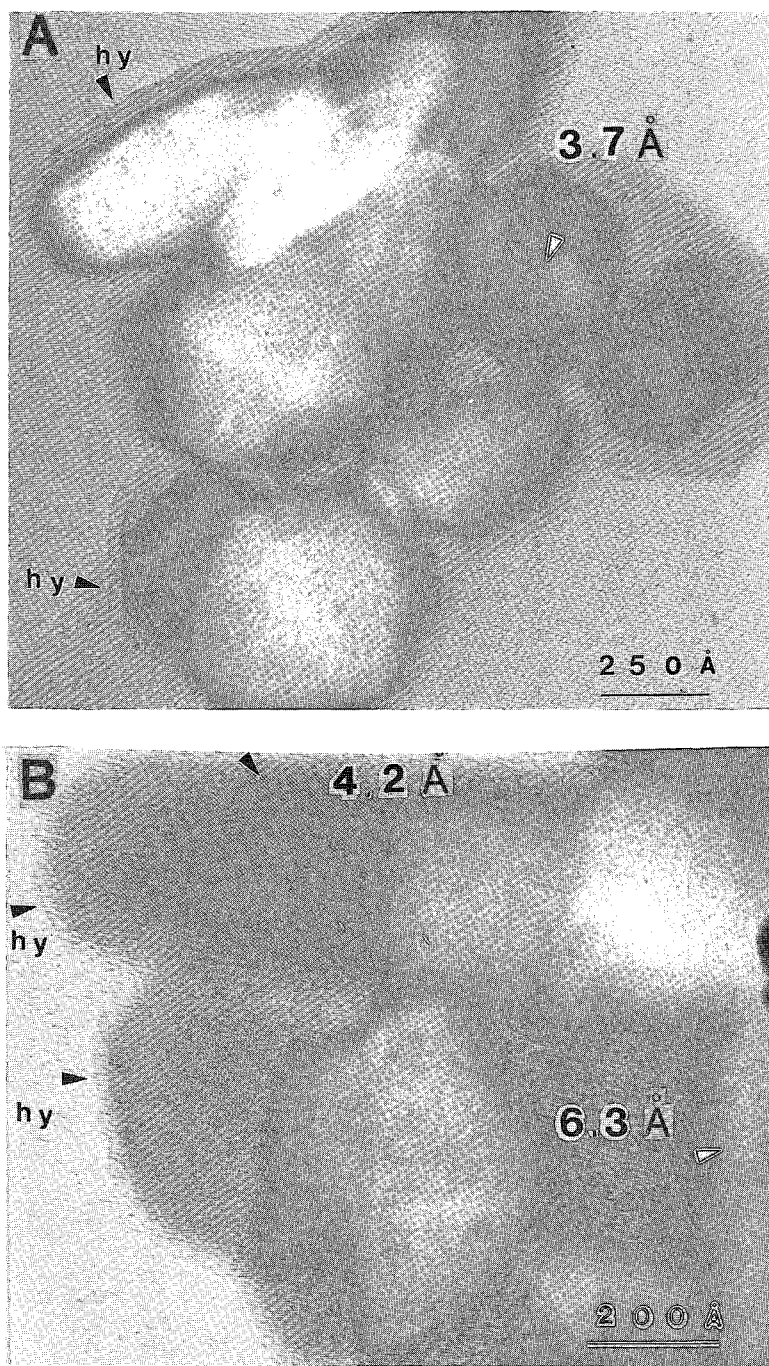


FIG. 9. High-resolution transmission electron micrographs of embryonic size of jarosite (A) and lath-shaped gypsum (B) crystals, showing lattice fringes of characteristic d values. hy: hydrated or amorphous thin film.

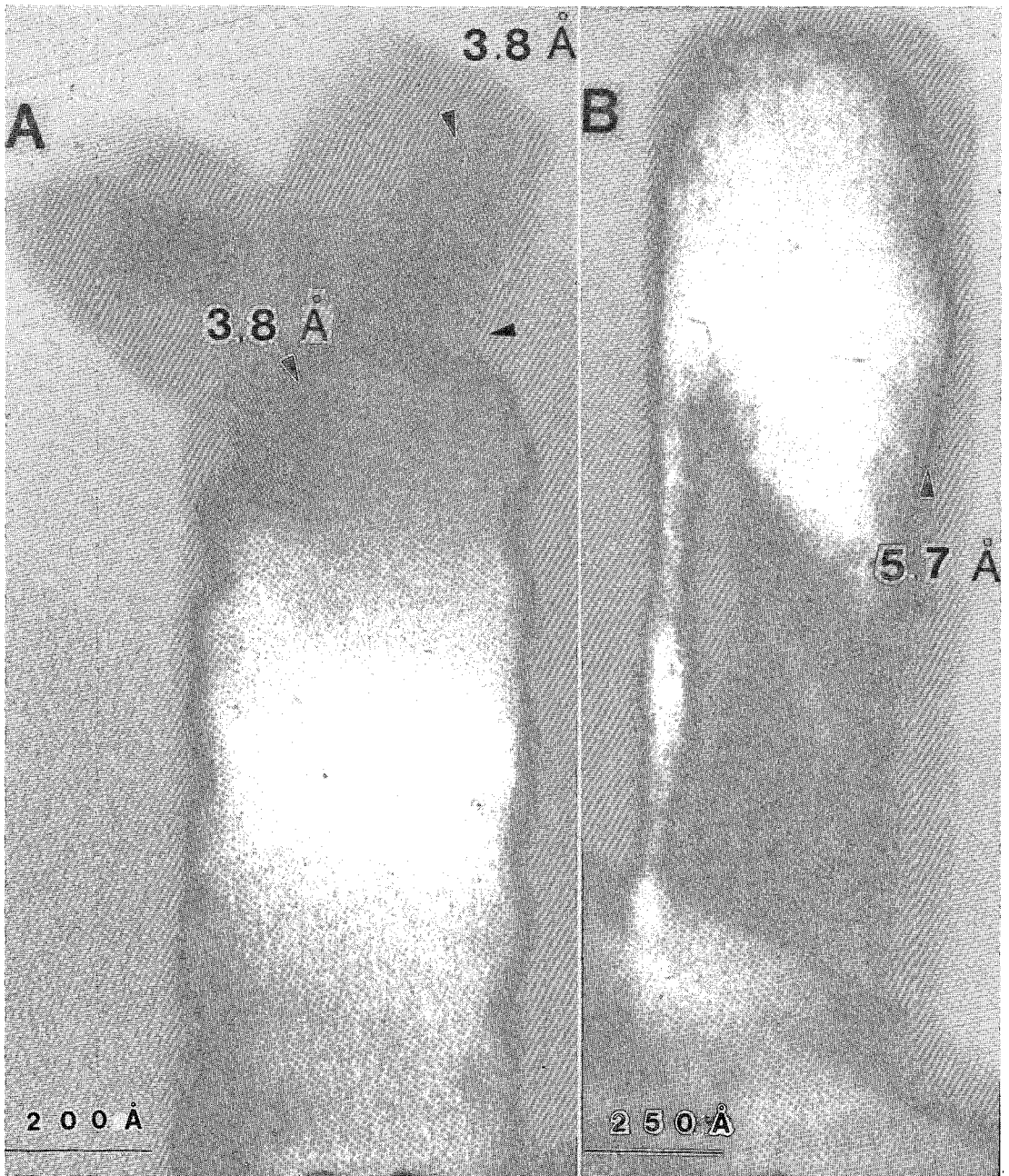


FIG. 10. High-resolution transmission electron micrographs of gypsum showing embryonic crystal with 3.8 Å spacing (A) and elongate lath-shaped crystal of jarosite with a d value of 5.7 Å (B).

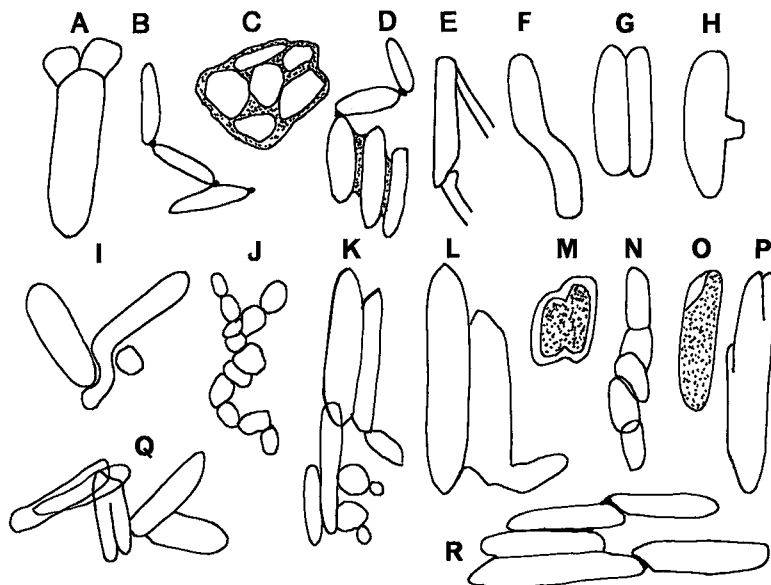


FIG. 11. Schematic summary of patterns of growth of embryonic crystals of both jarosite and gypsum, showing various patterns of division. An approximate scale is 2000–3000 Å long and 200–500 Å wide.

embryonic matter coated with hydrated thin films is essentially crystalline, having layer spacings typical of jarosite and gypsum. The morphology and connectivity of the crystals (Figs. 8–11) that were cultivated on the AT medium (Fig. 5–7) are variable. The division of a rod-shaped crystal was shown in lattice images. *T. thiooxidans* is important in catalyzing the oxidation of concrete to form jarosite. Under laboratory conditions that simulate low-temperature sediment diagenesis, elemental sulfur interacted with metal-loaded bacterial cells to form a variety of crystalline metal sulfides (Beveridge *et al.* 1983). This type of crystallization of jarosite and gypsum is stimulated by bacterial activity during oxidation of the iron sulfides to form sulfates in the corrosion of Portland cement concrete.

ACKNOWLEDGEMENTS

This work was supported by grants from the Monbusho (Ministry of Science, Culture and Education of Japan) (01430010) to Kazue Tazaki. Very useful assistance and comments by Drs. C.N. Alpers, R.F. Martin, and an anonymous referee also are gratefully acknowledged.

REFERENCES

- ALPERS, C.N. & BRIMHALL, G.H. (1989): Paleohydrologic evolution and geochemical dynamics of cumulative supergene metal enrichment at La Escondida, Atacama Desert, northern Chile. *Econ. Geol.* **84**, 229–255.
- _____, NORDSTROM, D.K. & BALL, J.W. (1989): Solubility of jarosite soil solutions precipitated from acid mine waters, Iron Mountain, California, U.S.A. *Sciences Géologiques* **42**, 281–298.
- _____, RYE, R.O., NORDSTROM, D.K., WHITE, L.D. & KING, BI-SHIN (1991): Chemical, crystallographic, and stable isotopic properties of alunite and jarosite from acid-hypersaline Australian lakes. *Chem. Geol.* **96**, 203–226.
- BEVERIDGE, T.J., MELOCHE, J.D., FYFE, W.S. & MURRAY, R.G.E. (1983): Diagenesis of metals chemically complexed to bacteria. *Appl. Environ. Microbiol.* **45**, 1094–1108.
- BLOOMFIELD, C. & COULTER, J. K. (1973): Genesis and management of acid sulfate soils. *Adv. Agron.* **25**, 265–326.
- BROPHY, G.P. & SHERIDAN, M.F. (1965): Sulfate studies. IV. The jarosite natrojarosite – hydronium

- jarosite solid solution series. *Am. Mineral.* **50**, 1595-1607.
- IVARSON, K.C. (1973): Microbiologic formation of basic ferric sulfates. *Can. J. Soil Sci.* **53**, 315-323.
- _____, ROSS, G.J. & MILES, N.M. (1978): Alterations of micas and feldspars during microbial formation of basic ferric sulfates in laboratory. *Soil Sci. Soc. Am. J.* **42**, 518-524.
- _____, _____ & _____ (1979): The microbiological formation of basic ferric sulfates. II. Crystallization in presence of potassium-, ammonium-, and sodium-salts. *Soil Sci. Soc. Am. J.* **43**, 908-912.
- _____, _____ & _____ (1980): The microbiological formation of basic ferric sulfates. 3. Influence of clay minerals on crystallization. *Can. J. Soil Sci.* **60**, 137-140.
- _____, _____ & _____ (1982): Microbiological transformations of iron and sulfur and their applications to acid sulfate soils and tidal marshes. *In Acid Sulfate Weathering* (L. R. Hossner, ed.). *Soil Sci. Soc. Am., Spec. Publ.* **10**, 57-75.
- _____, & SOJAK, M. (1978): Microorganisms and ochre deposits in field drains of Ontario. *Can. J. Soil Sci.* **58**, 1-17.
- KRISHNAMURTI, G.S.R. & HUANG, P.M. (1989): Influence of Mn^{2+} and pH on the formation of iron oxides from ferrous chloride and ferrous sulfate solutions. *Clays Clay Miner.* **37**, 451-458.
- KRUMBEIN, W.E. (1983): *Microbial Geochemistry*. Blackwell Scientific Publ., Oxford, England.
- _____, & DAHANAYAKE, K. (1985): Iron ores from Precambrian to Recent accumulated by heterotrophic microbial mats - stromatolites. *Terra Cognita* **5**, 295-296.
- LACEY, D.T. & LAWSON, F. (1970): Kinetics of the liquid-phase oxidation of acid ferrous sulfate by the bacterium *Thiobacillus ferrooxidans*. *Biotech. Bioeng.* **12**, 29-50.
- LEADBEATER, B.S.C. & RIDING, R. (1986): Biomineralization in lower plants and animals. *The Systematic Association, Spec. Vol.* **30**. Clarendon Press, Oxford, U.K.
- MICHEL, F.A. & VAN EVERDINGEN, R.O. (1987): Formation of a jarosite deposit on Cretaceous shales in the Fort Norman area, Northwest Territories. *Can. Mineral.* **25**, 221-226.
- MORI, T., NONAKA, T., TAZAKI, K., KOGA, M., HIKOSAKA, Y. & NODA, S. (1992): Interactions of nutrients, moisture and pH on microbial corrosion of concrete sewer pipes. *Wat. Res.* **26**, 29-37.
- MOUM, J. & ROSENQVIST, I.T. (1959): Sulfate attack on concrete in the Oslo region. *J. Am. Concrete Inst.* **56**, 257-264.
- NEILSEN, P.H. & HUVITVED-JACOBSEN, T. (1988): Effect of sulfate and organic matter on the hydrogen sulfide formation in biofilms of filled sanitary sewers. *J. Water Pollution Control Federation* **60**, 627-634.
- NORDSTROM, D.K. (1982): Aqueous pyrite oxidation and the consequent formation of secondary iron minerals. *In Acid Sulfate Weathering* (L.R. Hossner, ed.). *Soil Sci. Am., Spec. Publ.* **10**, 37-56.
- PARKER, C.D. (1945): The corrosion of concrete. 2. The function of *Thiobacillus concretivorus* (nov. spe.) in the corrosion of concrete exposed to atmospheres containing sulfide. *Aust. J. Exp. Biol.* **23**, 91-98.
- POMEROY, R.D. (1970): Sanitary sewer design for hydrogen sulfide control. *Public Works* **130**, 93-98.
- SAMPEI, Y. (1991): CHN-corder technique. *Earth Sci. (Chikyu Kagaku)* **45**, 285-289.
- SAND, W. (1987): Importance of hydrogen sulfide, thiosulfate and methylmercaptan for growth of *Thiobacilli* during simulation of concrete corrosion. *Appl. Environ. Microbiol.* **53**, 1645-1648.
- _____, & BOCK, E. (1984): Concrete corrosion in the Hamburg sewer system. *Environ. Technol. Lett.* **5**, 517-528.
- SANTER, M., BOYER, J. & SANTER, V. (1959): *Thiobacillus novellus*. I. Growth on organic and inorganic media. *J. Bacteriol.* **78**, 197-202.
- SILVER, M., EHRLICH, H.L. & IVARSON, K.C. (1986): Soil mineral transformation mediated by soil microbes. *In Soil Mineral with Natural Organics and Microbes* (P.M. Huang & M. Schnitzer, eds.). *Soil Sci. Soc. Am., Spec. Publ.* **17**, 497-519.
- TAYLOR, B.E., WHEELER, M.C. & NORDSTROM, D.K. (1984): Isotope composition of sulfate in acid mine drainage as a measure of bacterial oxidation. *Nature* **308**, 538-541.
- TAZAKI, K., MORI, T., NONAKA, T. & NODA, S. (1990a): Formation of jarosite on corroded portland cement. *Clay Sci. Japan (Nendo Kagaku)* **30**, 91-100.
- _____, _____, _____ & _____ (1990b): Mineralogical investigation of microbially corroded concrete. 2. Microbial corrosion of mortar bar. *Clay Sci. Japan (Nendo Kagaku)* **30**, 178-186.
- TORMA, A.E. (1976): Biodegradation of chalcopyrite.

- In Proc. 3rd Intern. Biodeg. Symp.* (J.M. Sharpley & A.M. Kaplan, eds.). Appl. Science Publishers Ltd., London (937-946).
- TUOVINEN, O.H. & CARLSON, L. (1979): Jarosite in culture of iron oxidizing *Thiobacilli*. *Geomicrobiol. J.* **1**, 205-210.
- U.S. ENVIRONMENTAL PROTECTION AGENCY (1985): Design manual, order and corrosion control in sanitary sewage systems and treatment plans. *U.S. Environ. Protection Agency, Rep.* **625**, 1-85.
- VAN BREEMEN, N. (1988): Redox process of iron and sulfur involved in the formation of acid sulfate soils. *In Iron in Soil and Clay Minerals* (J.W. Stucki, B.A. Goodman & U. Schwertman, eds.). *NATO Adv. Study Inst., Ser. C* **217**, 825-841. D. Reidel Publ. Co., Dordrecht, Holland.
- WIESE, R.G. & FYFE, W.S. (1986): Occurrences of iron sulfides in Ohio coals. *Int. J. Coal. Geol.* **6**, 251-276.
- , POWELL, M.A. & FYFE, W.S. (1987): Spontaneous formation of hydrated iron sulfates on laboratory samples of pyrite and marcasite-bearing coals. *Chem. Geol.* **63**, 29-38.
- ZODROW, E.L. & McCANDLISH, K. (1978): Hydrated sulfates in the Sydney coalfield, Cape Breton, Nova Scotia. *Can. Mineral.* **16**, 17-22.

Received April 24, 1991, revised manuscript accepted August 21, 1991.